A Generalized Approach to Modal Filtering for Active Noise Control—Part I: Vibration Sensing

Nicholas C. Burgan, Scott D. Snyder, Nobuo Tanaka, and Anthony C. Zander

***Abstract*—Many techniques for controlling the noise radiated by large structures require a large number of inputs to the controller to produce global attenuation. Unfortunately, processing the large number of inputs required is often beyond the capabilities of current controllers. In attempting to overcome this problem, many researchers have adopted various modal-filtering-type techniques. Such techniques involve resolving a small number of important global quantities (traditionally structural modes) from a large number of sensor measurements. However, current approaches require detailed structural information at the design stage. Determining this for complex, real-world structures may be very difficult, preventing many techniques from going beyond the laboratory. The technique presented here outlines a new sensing system strategy, where the radiated sound field is decomposed using multipole radiation patterns, thereby alleviating the need for detailed structural information. Simulation and experimental results are presented.**

I. Introduction

VIBRATION of and sound radiation from "large" structures is a problem that affects many organizations in many ways: aerospace firms, submarine and ship builders, electrical power utilities, and heavy vehicle manufacturers are a few prominent examples. Noise and vibration problems affect employees, prospective customers, and the surrounding community.

Active noise and vibration control has been pursued in situations where passive techniques have proved ineffective. Applying active control techniques to large structures has commonly involved scaling up smaller laboratory systems, systems that aim to minimize sound pressure amplitude or vibration at a number of error sensor locations [1]–[3]. In attempting to achieve more global control, large numbers of error sensors have been used, resulting in large numbers of inputs to, and outputs from, the control law and associated tuning algorithm. The resulting systems are costly and difficult to tune. More importantly, they are often not successful in attenuating noise and vibration problems, as current controllers have trouble processing and attenuating large numbers of inputs [4].

When approaching the development of an active control system, two design ideals are: 1) to be able to measure, and so attenuate, an error criterion that is directly related to acoustic power or energy and 2) to minimize the number of input signals that must be handled by the controller. Scaling-up smaller active control systems in an attempt to tackle larger problems may achieve 1), but at the detriment of 2). Sophisticated sensing system design is critical if the two design ideals are to be balanced.

In an attempt to do this, some researchers have adopted variants of modal filtering for sensing system design [5]–[8]. Modal filtering is a process whereby a small number of important global quantities, normally modal amplitudes, are resolved from a large number of sensor signals. In this way, the controller has to work with only a small number of important global quantities, balancing the design ideals, simplifying control law design, and maximizing convergence speed of the tuning algorithm. Modal filtering was originally developed for vibration control [5], with the amplitude of structural modes chosen as the set of global system states. The amplitudes of the structural modes were a convenient choice, being orthogonal contributors to the total energy in a vibrating structure. Thus, reducing these quantities was guaranteed to give a reduction in the vibration levels of the structure.

The choice of global quantities to sense is not as straightforward in noise control, as structural modes are often not orthogonal contributors to the sound radiated by a structure [9], [10] (assuming that the source of the noise is a vibrating structure). Past work has based the sensing system design on combinations of structural modes that are orthogonal in terms of the radiated sound power. These combinations have been referred to as radiation modes [11], and reducing their amplitude resulted in a reduction of the radiated sound power. It is possible to design a sensing system for measurement of these quantities using point vibration sensors [10], [11] or distributed, shaped piezoelectric polymer sensors [12], [13]. Fig. 1 shows how a typical modal filtering system may work.

The drawback of the radiation mode approach is that the technique assumes detailed knowledge of the structure, such as shape and mode information. Obtaining this for a simple structure in a laboratory setting, such as a simply supported rectangular panel, is a simple exercise. Translating this to a practical noise problem, such as radiation from a large electrical substation transformer, is often not practical. The impracticality is compounded by the fact that the vibration characteristics of every one of these structures will be somewhat different. For example, a "custom" sensing system would have to be designed for every transformer.

The aim of the work to be presented here is to overcome this need for structural mode information, to base the sensing

Manuscript received February 15, 2002; revised October 3, 2002. The associate editor coordinating the review of this paper and approving it for publication was Prof. Gert Cauwenberghs.

N. C. Burgan, S. D. Snyder, and A. C. Zander are with the Department of Mechanical Engineering, Adelaide University, Adelaide, South Australia 5005, Australia (e-mail: nburgan@mecheng.adelaide.edu.au; scott.snyder@adelaide.edu.au; azander@mecheng.adelaide.edu.au).

N. Tanaka is with the Department of Production, Information and Systems Engineering, Tokyo Metropolitan Institute of Technology, Tokyo 191-0065, Japan (e-mail: ntanaka@cc.tmit.ac.jp).

Digital Object Identifier 10.1109/JSEN.2002.807770

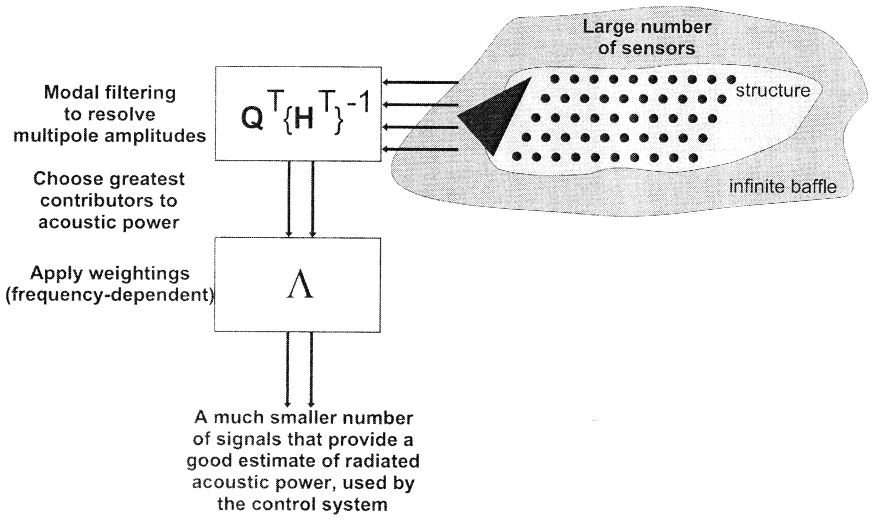

Fig. 1. Typical arrangement of a modal filtering system.

system design on quantities that are easily envisaged and generally transferable from structure to structure. The radiation patterns produced by acoustic multipoles will be used as a basis to describe the radiated acoustic power from the target structure, the multipoles being made up of (notional) arrays of acoustic monopoles. The idea of using acoustic multipoles is not new. It has been used previously in developing secondary acoustic sources for active noise control [14]–[19]. However, the aim here is different in that the radiation patterns produced by multipoles are used in the development of a sensing system.

In an associated paper [20] and in a previous paper [21], an approach for development of acoustic sensing systems was presented. In this paper, the same fundamental approach will be adapted for the design of vibration-based sensing systems, where the aim is attenuation of free field structural-acoustic radiation. An example of such a problem is noise radiation from an electrical transformer. Using structure-based (vibration) sensors in an active structural acoustic control system can offer a number of advantages over acoustic sensors located some distance away from the structure. For example, vibration sensors facilitate the development of a more physically compact control system. If the sensors and actuators are built into the structure, a "smart structure" can be produced [22]–[24]. Second, there is no acoustic propagation time delay in the system, often advantageous in control law design. Finally, the signals from structural sensors will not be as easily contaminated by contributions from extraneous noise sources such as wind.

The approach being taken here to sensing system design is fundamentally different to others presented previously in that the characteristics of a set of acoustic basis functions are being used to design a structural sensing system. Previous work has used structural basis functions to predict acoustic radiation. By reversing this world view, the need for detailed knowledge about the structure will be eliminated.

What will be presented here is an abbreviated derivation of the fundamental modal filtering problem. Much of the detailed rationale [21] and development for the acoustic sensing problem [20] has been presented elsewhere and so will not be repeated. The focus here will be to use the approach to develop a design methodology for vibration sensing systems. Simulation and experimental results for a simple problem will then be presented.

II. Theoretical Development

A. Development of a Quadratic Performance Measure

To develop a sensing system as described in the introduction, where a small number of global quantities are extracted from a large number of point measurements, it will prove to be beneficial to express the global performance measure J as a quadratic function

$$J(t, \omega) = \mathbf{q}^H(t)\mathbf{A}(\omega)\mathbf{q}(t). \tag{1}$$

In (1), $\mathbf{q}$ is a vector of (global) quantities to be measured, $\mathbf{A}$ is a positive definite, Hermitian weighting matrix, which in general will be frequency-dependent, and H indicates the Hermitian operation. Starting with a quadratic performance matrix also has intrinsic appeal for subsequent control law design.

The frequency-dependent weighting factors in $\mathbf{A}$ can be used as a guide in truncation of the problem, as these factors quantify how efficiently a particular state in $\mathbf{q}$ contributes to the global performance measure. Control law design will be simplified when the states are independent contributors to the error criterion, because if the controller works to reduce the amplitude of one state, the overall criterion will reduce. If $\mathbf{A}$ is diagonal, the system states in $\mathbf{q}$ are then independent contributors to the global performance measure.

In free space noise control, acoustic power is a common global performance measure. The aim of the exercise in this section is to express acoustic power as a quadratic error criterion without knowledge of the vibrational characteristics of the structure. Measurement of the states used in the resulting error criterion statement is then the target of the sensing system.

In this development, it will be assumed that the sound source is planar and radiating into a half space, as shown in Fig. 2.

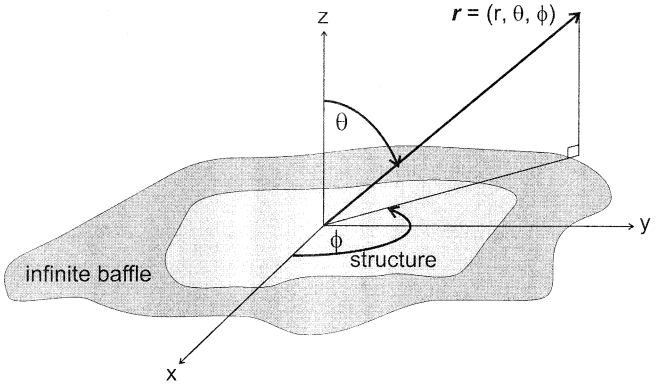

Fig. 2. Geometry for planar structure acoustic radiation.

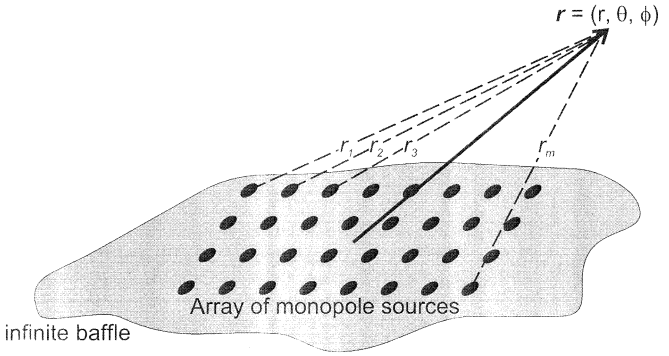

Fig. 3. An array of monopole sources used to derive multipole patterns.

However, the same development could be carried out for radiation into another type of space, for example, an enclosure. The important point to note is that there is no reliance on the structural information.

Consider then a planar sound source, situated in an infinite baffle, subject to harmonic excitation and radiating into free space, as shown in Fig. 2. The acoustic power W radiated by the structure can be evaluated by integrating the far-field acoustic intensity over a hemisphere enclosing the structure. Using the geometry of Fig. 2, this can be expressed as

$$W = \int_0^{2\pi} \int_0^{\pi/2} \frac{|p(\mathbf{r})|^2}{2\rho_0 c_0} |\mathbf{r}|^2 \sin(\theta)\, d\theta\, d\varphi \tag{2}$$

where $p(\mathbf{r})$ is the acoustic pressure at location $\mathbf{r}$ in space, where the location is defined by $\mathbf{r} = (r, \theta, \phi)$. The terms ρ_0 and c_0 are the density of air and the speed of sound in air, respectively.

For the development here, let the pressure be decomposed using the radiation patterns produced by acoustic multipoles as a basis, in the same way that structural velocity can be decomposed using structural mode shape functions as a basis. As such, we can write

$$p(\mathbf{r}) = \sum_{i=1}^{\infty} a_i \psi_i(\mathbf{r}) \tag{3}$$

where a_i is the amplitude of the ith multipole and $\psi_i(\mathbf{r})$ is the radiation transfer function for the ith multipole, between the origin and the location $\mathbf{r}$ (i.e., the value of the radiation pattern generated by the multipole at location $\mathbf{r}$ in space). The multipole radiation patterns used in this exercise will be derived from an array of in-phase and out-of-phase monopoles on the structure surface. Such an arrangement is shown in Fig. 3. The radiation patterns produced by arrays of monopoles were chosen, rather than more conventional monopole, dipole, or quadrupole arrangements, as it allows for more flexibility in adapting the technique to different situations. Using just monopoles, the array can be easily expanded to cover a surface of any shape and area, allowing the technique to be used in a sensing system for controlling the sound radiated from any type of structure. The exact geometry and extent of the array used will be problem-specific, with its selection dependent on such factors as size and geometry of the structure under consideration and the frequency range of interest. A specific example will be presented later in this paper.

The pressure field radiated by a baffled monopole at any point in space is given by

$$p(\mathbf{r}) = q \frac{j\omega\rho_0}{2\pi r} e^{-jkr} \tag{4}$$

where q is the volume velocity of the monopole, k is the acoustic wavenumber ω/c_0, ω is the angular frequency of oscillation, and harmonic time dependence is assumed. For the development here, all of the monopoles within a multipole will be defined to have the same volume velocity amplitude, with phase of 0° or 180°. The amplitude a_i of the ith multipole will be defined as the volume velocity q of the monopoles which make up that multipole.

If the infinite sum in (3) is truncated at n acoustic multipoles, acoustic pressure can be expressed in matrix form as

$$p(\mathbf{r}) \approx \boldsymbol{\psi}(\mathbf{r})\mathbf{a} \tag{5}$$

where $\boldsymbol{\psi}(\mathbf{r})$ is a row vector whose elements are the values of the radiation transfer functions of the n multipoles included in the calculation, from the origin to the point $\mathbf{r}$, and is given by

$$\boldsymbol{\psi}(\mathbf{r}) = [\psi_1(\mathbf{r}) \quad \psi_2(\mathbf{r}) \quad \cdots \quad \psi_n(\mathbf{r})] \tag{6}$$

and $\mathbf{a}$ is a column vector whose elements are the complex amplitudes of the n multipoles

$$\mathbf{a} = \begin{bmatrix} a_1 \\ a_2 \\ \vdots \\ a_n \end{bmatrix}. \tag{7}$$

As an example of how the radiation transfer functions for the individual multipoles $\psi_n(\mathbf{r})$ are calculated, consider one of the n multipoles consisting of m monopoles which are all in phase. Using (4), the pressure produced by the multipole at point $\mathbf{r}$ in space would be

$$\begin{aligned} &p_{\text{multipole}}(\mathbf{r}) \\ &\quad = a_{\text{multipole}} \left(\frac{j\omega\rho_0}{2\pi r_1} e^{-jkr_1} + \frac{j\omega\rho_0}{2\pi r_2} e^{-jkr_2} + \cdots \right. \\ &\qquad \left. + \frac{j\omega\rho_0}{2\pi r_m} e^{-jkr_m} \right) \qquad (8) \\ &\quad = a_{\text{multipole}} \psi_{\text{multipole}}(\mathbf{r}) \qquad (9) \end{aligned}$$

where $a_{\text{multipole}}$ is the amplitude of the multipole

$$\psi_{\text{multipole}}(\mathbf{r}) = \frac{j\omega\rho_0}{2\pi r_1}\, e^{-jkr_1} + \frac{j\omega\rho_0}{2\pi r_2}\, e^{-jkr_2} + \cdots + \frac{j\omega\rho_0}{2\pi r_m}\, e^{-jkr_m} \quad (10)$$

and r_1, r_2, and r_m are the distances from the m monopoles which make up the multipole to the point $\mathbf{r}$ in space, as shown in Fig. 3.

If (5) is substituted into (2), the pressure term can be expanded to give

$$W \approx \int_0^{2\pi} \int_0^{\pi/2} \frac{\mathbf{a}^H \boldsymbol{\psi}^H(\mathbf{r})\boldsymbol{\psi}(\mathbf{r})\mathbf{a}}{2\rho_0 c_0} |\mathbf{r}|^2 \sin(\theta)\, d\theta\, d\varphi \quad (11)$$

which can be written as

$$W \approx \mathbf{a}^H \mathbf{A}_a \mathbf{a} \quad (12)$$

where $\mathbf{A}_a$ is a square weighting matrix, whose (i, j)th term is given by

$$\mathbf{A}_a(i, j) = \int_0^{2\pi} \int_0^{\pi/2} \frac{\psi_i^*(\mathbf{r})\psi_j(\mathbf{r})}{2\rho_0 c_0} |\mathbf{r}|^2 \sin(\theta)\, d\theta\, d\varphi \quad (13)$$

where the ψ_i and ψ_j terms are calculated using the same method as was used to derive (10). Note that they are dependent on the geometry of the multipoles and frequency but require no structural knowledge.

Equation (12) has the desired form which was presented in (1). As expected, the weighting matrix will be frequency-dependent.

As discussed, ideally $\mathbf{A}_a$ would be diagonal, meaning that the multipoles were independent contributors to the performance measure. For a particular choice of multipoles this may not be the case. However, $\mathbf{A}_a$ will be symmetric and can be diagonalized using an orthonormal transformation, as described shortly.

As a specific example, consider the radiation patterns from an array of eight monopole sources, as shown in Fig. 4. To produce each multipole pattern, the amplitude of the monopoles were chosen to be equal, while the phase relationship of the monopoles is described by (14), shown at the bottom of the page, where $\psi_1(\mathbf{r})$–$\psi_8(\mathbf{r})$ are the transfer functions from multipoles 1–8 to the position $\mathbf{r}$, and r_1–r_8 are the distances from the eight monopoles to the position $\mathbf{r}$. As can be seen, the first multipole pattern is generated by having all of the sources in phase, the second by having sources 1–4 in phase and 5–8 out of phase, the third by having sources 1, 2, 7, and 8 in phase and 3–6 out of phase, etc. The "phasing" matrix in (14) contains a set of orthogonal rows (and columns) composed of ± 1, and is referred to as a Hadamard matrix $\mathbf{H}$. Hadamard matrices can be generated of any size 2^n by 2^n for any integer n [25]. They have been used previously in the study of vibration transmission [26].

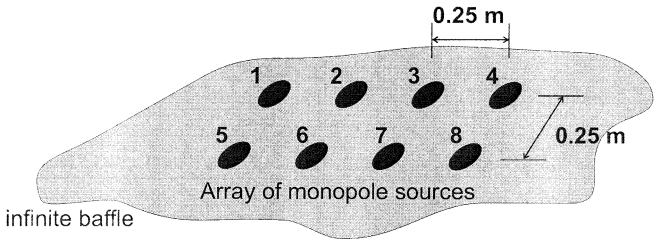

Fig. 4. Specific multipole arrangement to be considered.

B. Evaluation of Multipole Amplitudes Using Vibration Sensors

Consider now the estimation of the multipole amplitudes used to model the acoustic space by measurement of vibration on the structure surface. If the structural velocity was measured at one of the notional monopole positions, then its value would effectively be the superposition of the volume velocities of the eight monopoles at that point (one from each multipole). Consider measurement of the structural velocity at the position of the third monopole (see Fig. 4). Recall that the phase relationship within the multipoles is defined by the *rows* of a Hadamard matrix, $\mathbf{H}$ in (14). As such, the *columns* of $\mathbf{H}$ give the phase relationship between the monopoles at a particular position. Thus, we can write

$$vel(3) = 1.a_1 + 1.a_2 - 1.a_3 - 1.a_4 - 1.a_5 + 1.a_6 + 1.a_7 - 1.a_8 \quad (15)$$

$$= [1 \quad 1 \quad -1 \quad -1 \quad -1 \quad 1 \quad 1 \quad -1]\mathbf{a} \quad (16)$$

where $vel(3)$ is the structural velocity at position 3, a_1–a_8 are the amplitudes of the multipoles (the amplitude of a multipole is

$$\begin{bmatrix} \psi_1(\mathbf{r}) \\ \psi_2(\mathbf{r}) \\ \psi_3(\mathbf{r}) \\ \psi_4(\mathbf{r}) \\ \psi_5(\mathbf{r}) \\ \psi_6(\mathbf{r}) \\ \psi_7(\mathbf{r}) \\ \psi_8(\mathbf{r}) \end{bmatrix} = \frac{j\omega\rho_0}{2\pi} \begin{bmatrix} 1 & 1 & 1 & 1 & 1 & 1 & 1 & 1 \\ 1 & 1 & 1 & 1 & -1 & -1 & -1 & -1 \\ 1 & 1 & -1 & -1 & -1 & -1 & 1 & 1 \\ 1 & 1 & -1 & -1 & 1 & 1 & -1 & -1 \\ 1 & -1 & -1 & 1 & -1 & 1 & 1 & -1 \\ 1 & -1 & 1 & -1 & -1 & 1 & -1 & 1 \\ 1 & -1 & 1 & -1 & 1 & -1 & 1 & -1 \\ 1 & -1 & -1 & 1 & 1 & -1 & -1 & 1 \end{bmatrix} \begin{bmatrix} \frac{e^{-jkr_1}}{r_1} \\ \frac{e^{-jkr_2}}{r_2} \\ \frac{e^{-jkr_3}}{r_3} \\ \frac{e^{-jkr_4}}{r_4} \\ \frac{e^{-jkr_5}}{r_5} \\ \frac{e^{-jkr_6}}{r_6} \\ \frac{e^{-jkr_7}}{r_7} \\ \frac{e^{-jkr_8}}{r_8} \end{bmatrix} = \frac{j\omega\rho_0}{2\pi}\mathbf{H} \begin{bmatrix} \frac{e^{-jkr_1}}{r_1} \\ \frac{e^{-jkr_2}}{r_2} \\ \frac{e^{-jkr_3}}{r_3} \\ \frac{e^{-jkr_4}}{r_4} \\ \frac{e^{-jkr_5}}{r_5} \\ \frac{e^{-jkr_6}}{r_6} \\ \frac{e^{-jkr_7}}{r_7} \\ \frac{e^{-jkr_8}}{r_8} \end{bmatrix} \quad (14)$$

defined as being the amplitude of the monopole sources which comprise it), and

$$\mathbf{a} = \begin{bmatrix} a_1 \\ a_2 \\ \vdots \\ a_8 \end{bmatrix}. \tag{17}$$

The ± 1 terms correspond to those in the third column of the Hadamard matrix $\mathbf{H}$.

This process is similar to the way in which the vibration at a point can be derived from structural modal amplitudes. The vibration at a point is equal to the sum of the product of the value of the mode shape functions at the point and the modal amplitudes, that is,

$$\begin{aligned} &[\text{vibration at a point}] \\ &= [- \quad \text{values of mode shape functions} \quad -] \\ &\cdot \begin{bmatrix} | \\ \text{modal} \\ \text{amplitudes} \\ | \end{bmatrix}. \end{aligned} \tag{18}$$

In the technique proposed here, the elements of the Hadamard matrix perform the same operation as the mode shape functions in a traditional analysis. Equations similar to (16) can be written at all other monopole positions, and the equations can be combined into a single matrix equation

$$\mathbf{vel} = \mathbf{H}^T\mathbf{a} \tag{19}$$

where

$$\mathbf{vel} = \begin{bmatrix} vel(1) \\ vel(2) \\ \vdots \\ vel(8) \end{bmatrix}$$

and $vel(1)$–$vel(8)$ represent the structural velocity measurements at the positions of the eight monopoles.

From (19), it is possible to resolve the multipole amplitudes, from vibration measurements, using a matrix inversion

$$\mathbf{a} = \{\mathbf{H}^T\}^{-1}\mathbf{vel}. \tag{20}$$

Equation (20) has the form of a standard modal filtering problem [7]. Note that a $n \times n$ Hadamard matrix satisfies the property that $\mathbf{H}.\mathbf{H}^T = n.\mathbf{I}$ [27]. Thus, the inverse of the transpose of the Hadamard matrix is equal to the Hadamard matrix itself scaled by the inverse of the size of the Hadamard matrix (the number of multipoles)

$$\{\mathbf{H}^T\}^{-1} = \frac{1}{n}\mathbf{H}. \tag{21}$$

III. Sensing System Development

The aim here is to develop a sensing system in which a large number of sensor measurements are resolved into a small number of global signals, from which the global performance measure can be determined, as is shown in Fig. 1. If we substitute (20) into (12), acoustic power can be described as

$$W \approx \mathbf{vel}^H\{\{\mathbf{H}^T\}^{-1}\}^H\mathbf{A}_a\{\mathbf{H}^T\}^{-1}\mathbf{vel}. \tag{22}$$

In (22), the vibration measurements are resolved into multipole amplitudes by the $\{\mathbf{H}^T\}^{-1}$ terms (which act like modal filters). The multipole amplitudes are then weighted by the $\mathbf{A}_a$ matrix to give the total radiated acoustic power.

At this stage, it is important to consider how such a system could be implemented in practice. Referring to Fig. 1, if, for example, an adaptive feedforward control system was to be used, the large number of vibration signals would be decomposed by $\{\mathbf{H}^T\}^{-1}$ into the multipole amplitudes, as with a standard modal filtering problem. The multipoles with the highest radiation efficiencies could be selected through consideration of the terms in $\mathbf{A}_a$ and the reduced number of signals corresponding to these multipoles could then be passed through filters having frequency characteristics defined by the terms in $\mathbf{A}_a$, which would take into account their relative importance before being fed to the control algorithm [28]. If feedback control were to be used, the resolved multipole amplitudes would be used as the error criteria for the controller and the weighting terms could be incorporated into the control system through a number of ways. See, for example, [29]–[31].

For practical implementation of such a system, there are two points which must be addressed.

- **Are the multipoles independent contributors to radiated acoustic power?** The multipoles will only be independent contributors to power if $\mathbf{A}_a$ is diagonal. If the inputs to the controller are not independent, then a reduction in one of them will not necessarily result in a reduction of the global performance measure.
- **How many multipoles are required to adequately model an arbitrary sound field?** The sizes of the terms in $\mathbf{A}_a$ determine the relative contributions that the multipoles make to the global performance measure. The largest contributors can be taken as sufficient to model a sound field.

Consider the first of the questions posed above: is the weighting matrix $\mathbf{A_a}$ diagonal? In fact, while the rows of the Hadamard matrix defining the phase relationship of the monopoles within each multipole are orthogonal, the radiation patterns produced by the eight multipoles are not. For example, for the multipole geometry of Fig. 4, at 100 Hz the terms in the matrix are shown in (23), at the bottom of the next page, with the order of the multipoles (1–8) being the order of the rows in the defining matrix in (14). The off-diagonal elements in (23) quantify the cross coupling between the various multipole radiation patterns. The pattern of cross coupling is similar to that seen when calculating the acoustic power radiated from a simply supported rectangular panel in terms of vibration modes [28]. For example, the first multipole is similar to a (1, 1) panel structural mode, the eighth multipole is similar to a (3, 1) panel mode, and the cross coupling between the multipoles [quantified by the (8, 1) or (1, 8) elements in the matrix in (23)] is similar to the cross coupling between the panel modes.

As $\mathbf{A_a}$ is symmetric, it can be diagonalized using an orthonormal transformation [32]

$$\mathbf{A_a} = \mathbf{Q}\mathbf{\Lambda}\mathbf{Q}^T \tag{24}$$

where $\mathbf{Q}$ is a unitary matrix whose columns are the eigenvectors of $\mathbf{A_a}$, and $\mathbf{\Lambda}$ is a diagonal matrix whose elements are the associated eigenvalues. Substituting this into (22) yields

$$W \approx \mathbf{vel}^H\{\{\mathbf{H}^T\}^{-1}\}^H\mathbf{Q}\mathbf{\Lambda}\mathbf{Q}^T\{\mathbf{H}^T\}^{-1}\mathbf{vel}. \quad (25)$$

The eigenvalues of $\mathbf{A_a}$ plotted as a function of frequency in the range 25–250 Hz are shown in Fig. 5. The associated eigenvector matrix at 100 Hz is given in (26), shown at the bottom of the page, where the eigenvectors (columns) are arranged in order of decreasing (corresponding) eigenvalue.

Consider now the second question posed, that of how many multipoles are required to adequately model a given sound field. With $\mathbf{A_a}$ subject to an orthonormal transformation, it is now the magnitude of the eigenvalues in $\mathbf{\Lambda}$ for a given frequency that provides the answer, as these eigenvalues are effectively the radiation efficiencies of orthogonal combinations of multipoles. Observe from Fig. 5 that, over most of the frequency range of interest, the radiation efficiencies of three of the multipole combinations (from the eigenvector matrix in (26), essentially multipoles 6, 7, and 8) are significantly below the others. This suggests that reasonable modeling of the sound field will be obtained by considering only the first five multipole combinations, as defined by the first five columns of the eigenvector matrix in (26). It follows that reasonable sound field attenuation may be achieved by implementing a sensing system that resolves and attenuates only the first five multipole combinations. Hence, a five-input control system would be required.

Equation (25) is of the desired form as described in (1). The multipole amplitudes are resolved from a number of sensor measurements using $\{\mathbf{H}^T\}^{-1}$, and orthogonal groupings of the multipoles are then formed using $\mathbf{Q}$. So together $\{\mathbf{H}^T\}^{-1}$ and $\mathbf{Q}$ form the modal filter weights. The former is frequency-independent and the latter has a weak frequency dependence which can be ignored (i.e., the values from a particular frequency can be used). *Thus, the modal filter weights can be approximated as fixed values* when implementing the sensing system. The terms of the diagonal matrix $\mathbf{\Lambda}$ weight the transformed multipoles according to their relative contributions to the radiated acoustic power. As seen in Fig. 5, the terms vary strongly with frequency, and their frequency dependence cannot be ignored. To implement this practically, in an adaptive feedforward arrangement, digital filters can be built with characteristics defined by the terms in $\mathbf{\Lambda}$. If required, a further simplification can be made. Observe in Fig. 5 that, although the terms in $\mathbf{\Lambda}$ vary with frequency, the ratios between them do not vary greatly. When adaptive feedforward control is used, it is the relative importance of the quantities, rather than their absolute values, which is important. Thus, the weights can also be approximated as fixed values.

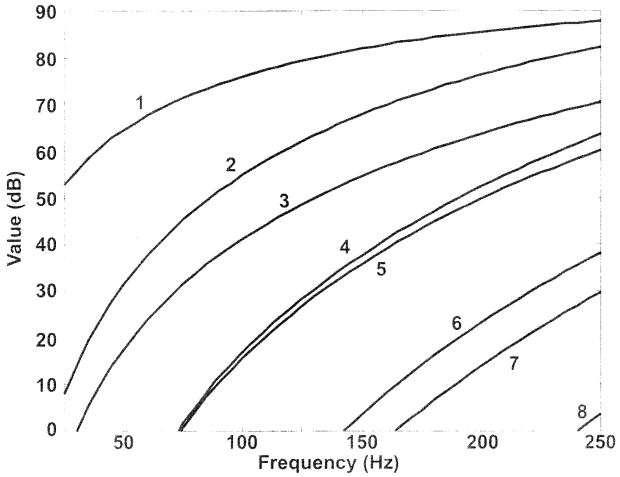

Fig. 5. Eigenvalues of the first eight eigenvectors $\mathbf{A_a}$, plotted as a function of frequency.

$$\mathbf{A_a}(100\text{ Hz}) = \begin{bmatrix} 6287.2 & 0 & 0 & 0 & 0 & 0 & 0 & -217.0 \\ 0 & 114.9 & 0 & 0 & -2.36 & 0 & 0 & 0 \\ 0 & 0 & 4.86 & 0 & 0 & 2.38 & 0 & 0 \\ 0 & 0 & 0 & 449.8 & 0 & 0 & 217.7 & 0 \\ 0 & -2.36 & 0 & 0 & 0.11 & 0 & 0 & 0 \\ 0 & 0 & 2.38 & 0 & 0 & 1.16 & 0 & 0 \\ 0 & 0 & 0 & 217.7 & 0 & 0 & 105.4 & 0 \\ -217.0 & 0 & 0 & 0 & 0 & 0 & 0 & 12.79 \end{bmatrix} \quad (23)$$

$$\mathbf{Q}(100\text{ Hz}) = \begin{bmatrix} 0.99 & 0 & 0 & 0 & 0.03 & 0 & 0 & 0 \\ 0 & 0 & 0.99 & 0 & 0 & 0.02 & 0 & 0 \\ 0 & 0 & 0 & 0.90 & 0 & 0 & 0 & -0.44 \\ 0 & 0.90 & 0 & 0 & 0 & 0 & -0.43 & 0 \\ 0 & 0 & -0.02 & 0 & 0 & 0.99 & 0 & 0 \\ 0 & 0 & 0 & 0.44 & 0 & 0 & 0 & 0.89 \\ 0 & 0.44 & 0 & 0 & 0 & 0 & 0.90 & 0 \\ -0.03 & 0 & 0 & 0 & 0.99 & 0 & 0 & 0 \end{bmatrix} \quad (26)$$

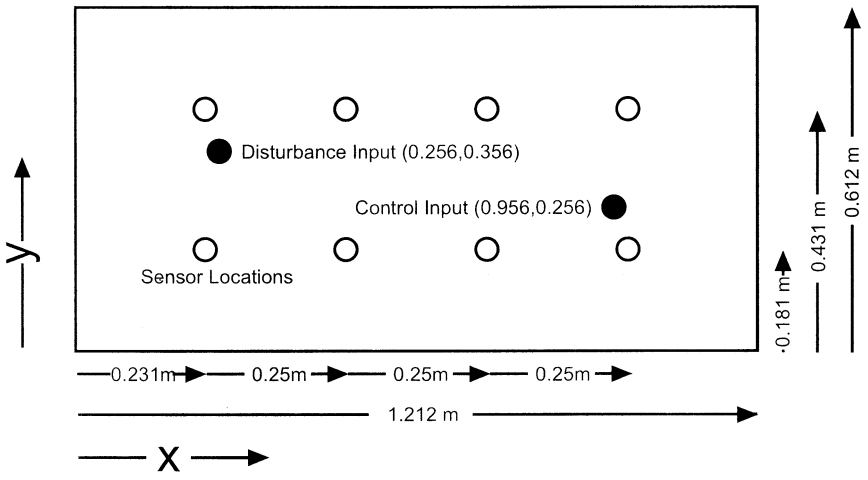

Fig. 6. Schematic diagram of the panel.

The resulting sensing system can be implemented very easily.

1) Measure the structural velocity at the measurement locations.
2) Multiply the vector of structural velocity measurements by the fixed terms in $\{\mathbf{H}^T\}^{-1}$ and $\mathbf{Q}$ (resulting in a greatly reduced number of outputs).
3) Pass the small number of resulting signals through a set of filters with characteristics defined by $\mathbf{\Lambda}$ or, as a further simplification, multiply them by another fixed set of weights to account for the relative sizes of the terms in $\mathbf{\Lambda}$.
4) Finally, the resulting signals are input to the controller.

IV. Simulation

To evaluate the effectiveness of the proposed technique, numerical simulations were performed. The problem of controlling the sound radiated by a simply supported, rectangular, baffled, steel panel was considered. Referring to Fig. 6, the panel had dimensions 1.212 m (L_x) by 0.612 m (L_y) with a thickness of 0.004 m. The panel was excited by a disturbance point force located at $x = 0.256$, $y = 0.356$, and a single control point force was considered, located at $x = 0.956$, $y = 0.256$. In calculating the response of the panel, the first 51 structural modes of the panel were considered. The frequency range of interest was up to 250 Hz, a range which includes the first ten natural frequencies of the panel, which are listed in Table I.

The sensing system used in the simulation consisted of an array of eight structural velocity sensors attached to the panel. The positions of the sensors were chosen to correspond to the positions of the monopole elements that make up the multipoles. This resulted in sensors with locations given in Table II.

The aim of the simulation here is to investigate how much power reduction is achievable by minimizing different numbers of multipoles and comparing these values to the maximum possible power reduction using the given control force location (see [33] for a description of how to calculate this). An open-loop feedforward approach is used here. It must be emphasized that the aim of the exercise is to examine the quality of the sensing system design approach: how close to the theoretical optimum result will this sensing system take the controller.

TABLE I
First Ten Natural Frequencies of the Panel

Mode	Natural Frequency (Hz)
1,1	33.0
2,1	53.1
3,1	86.6
1,2	111.8
2,2	131.9
4,1	133.5
3,2	165.4
5,1	193.8
4,2	212.3
1,3	243.2

TABLE II
Structural Velocity Sensor Locations

Accelerometer Number	x - position (m)	y - position (m)
1	0.231	0.431
2	0.481	0.431
3	0.731	0.431
4	0.981	0.431
5	0.231	0.181
6	0.481	0.181
7	0.731	0.181
8	0.981	0.181

The expression for radiated sound power on which this technique is based is shown in (25). The approximation for radiated acoustic power is effectively a weighted sum of the structural velocity signals. The Hadamard matrix $\{\mathbf{H}^T\}^{-1}$ resolves the multipole amplitudes from the structural velocity signals. The eigenvectors of the $\mathbf{A}_a$ matrix $\mathbf{Q}$ resolves orthogonal combinations of the multipoles, and $\mathbf{\Lambda}$, which contains the eigenvalues of the $\mathbf{A}_a$ matrix, weights the orthogonal combinations of multipoles according to their relative contributions to radiated acoustic power.

To simulate a technique that can be practically implemented, fixed values of the weakly frequency-dependent terms were used. In (25), $\mathbf{Q}$, and $\mathbf{\Lambda}$ are frequency-dependent. In the simulation, the values at 100 Hz were used for all frequencies.

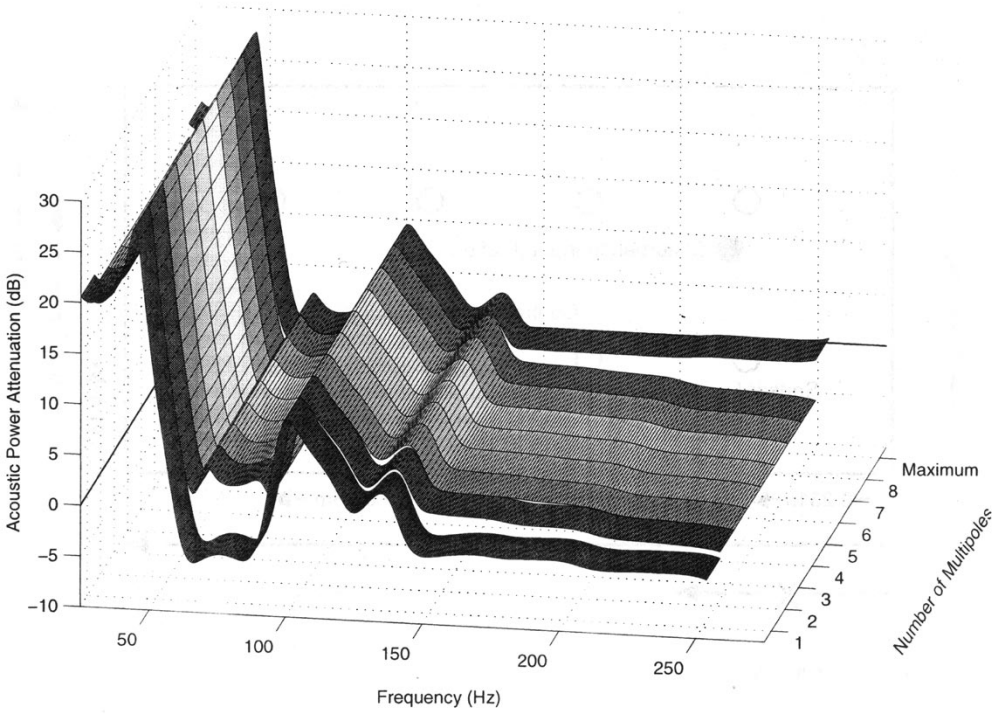

Fig. 7. Comparison of minimizing 1–8 multipoles.

It is important to keep in mind that the sensing system has been designed without *a priori* knowledge of the mode shapes of the structure. Equation (25) is an approximation to the radiated acoustic power as it has been truncated. In theory, if an infinite number of multipoles were used, the expression would be equivalent to the true power. The number of multipoles to be included is chosen by examining the associated eigenvalues, which represent the relative contribution of a multipole to radiated acoustic power. Only multipoles with eigenvalues above 0.1% of the maximum eigenvalue are included.

The amount of power attenuation achievable by including a certain number of multipoles in the analysis can be calculated by using quadratic optimization [33], [34] on (25). In (25), the structural velocity signals $\mathbf{vel}$ can be expressed in terms of the primary and control forces on the panel. It is then possible to find the value of the control force that will minimize the value of the expression, i.e., the minimum power. The attenuation achievable is given by the difference between the radiated acoustic power from the panel when the primary force is operating in isolation and when the primary and control forces are operating together.

Quadratic optimization was performed using various numbers of multipoles. The attenuation achievable using the given control force location, and including one to eight multipoles, is shown in Fig. 7. Also shown in the figure is the maximum attenuation possible using the given control force configuration. To calculate the maximum possible attenuation, the following expression for power is used:

$$W = \mathbf{v}^H \mathbf{A} \mathbf{v} \tag{27}$$

where $\mathbf{v}$ is the vector of modal velocity amplitudes, and $\mathbf{A}$ is the "power transfer matrix." The derivation of (27) is given in [35]. Quadratic optimization can be used on (27) in the same way as described above, by expressing the modal velocity amplitudes in terms of the control force.

Several features are important to observe in Fig. 7. First, there is a considerable increase in the attenuation achievable by minimizing two multipoles instead of one. There is a smaller benefit obtained in minimizing three multipoles over two, but, for this configuration, very little further improvement is seen in increasing the number of multipoles considered from three to eight.

Since the maximum amount of attenuation possible is nearly achieved using just three multipoles, it is sensible to resolve just three multipoles. In doing this, eight sensor signals are resolved into three error signals to be input to the controller. By reducing the number of inputs to a controller, its design is simplified and convergence speed is maximized [36].

Second, when minimizing eight multipoles, the attenuation achievable at low frequencies is approximately equivalent to the maximum attenuation possible with the given control force location. The attenuation achievable at higher frequencies when minimizing eight multipoles is less than the maximum possible attenuation. This is due to inaccuracies in resolving the multipoles with only eight sensors, as it has been shown elsewhere [21] that eight accurately described multipoles will give the maximum achievable result in this range.

V. Experimental Verification

Experiments were conducted to verify the theory and simulations presented in the previous sections. The aim was to closely mimic the optimal open loop control law to minimize the sensing system output, and then assess the resultant level of acoustic power attenuation.

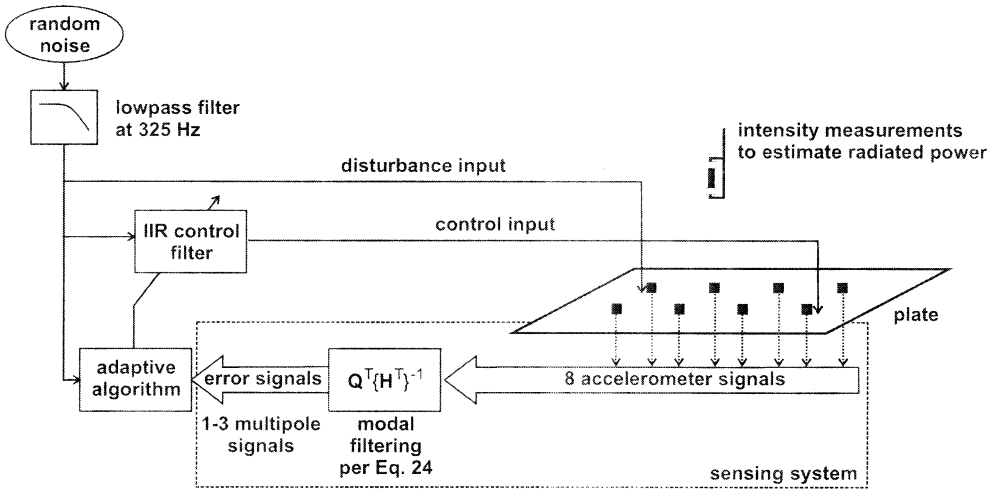

Fig. 8. Schematic representation of the experimental arrangement.

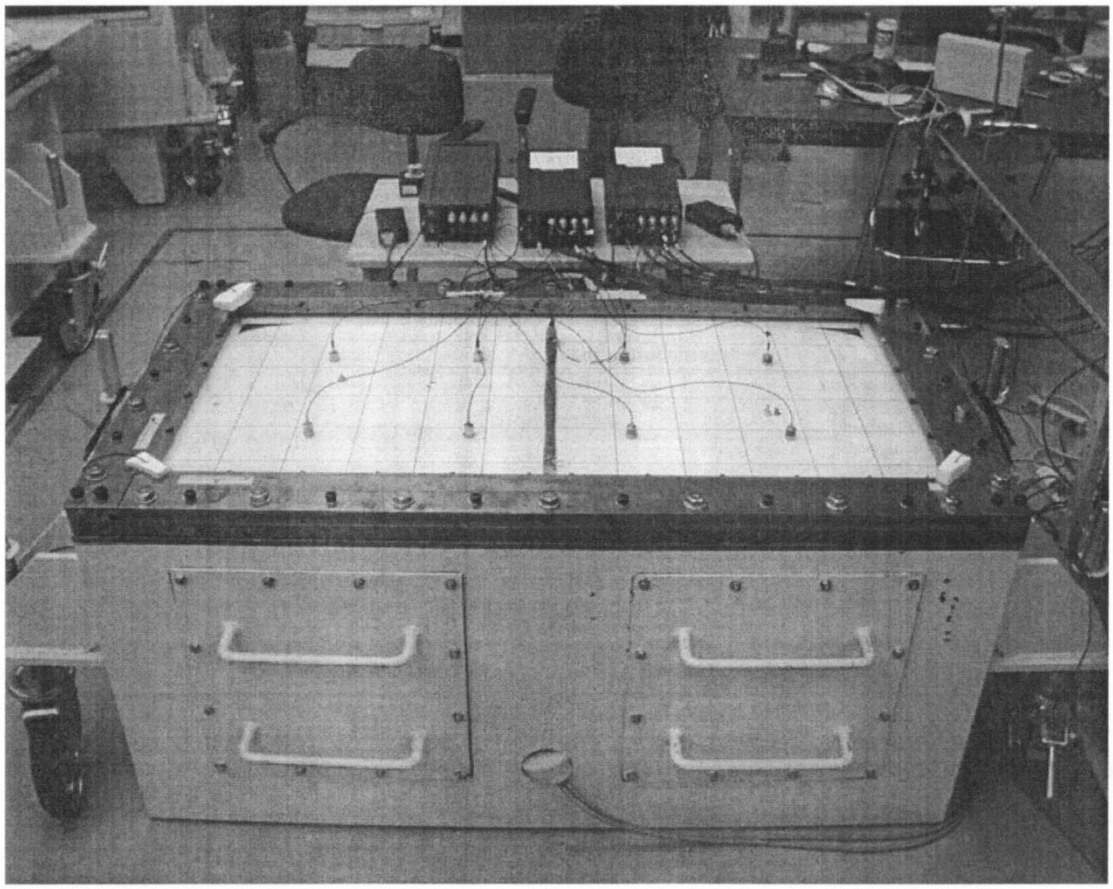

Fig. 9. Experimental arrangement, showing the panel and accelerometers.

A. Experimental Setup

Referring to Fig. 8, a rectangular steel panel the same dimensions as in the simulation, 1.212 m by 0.612 m and a thickness 0.004 m, was fixed in a steel base designed to provide simply supported boundary conditions. Two electrodynamic shakers were attached to the panel, one used as the disturbance and the other as the control input. The shakers were located in the same positions as in the simulations described previously. Structural velocity was measured by integrating the signals from eight accelerometers attached to the plate, at the same locations as those used in the simulations described previously (Table II). The disturbance input was random noise, low-pass filtered at 325 Hz.

Adaptive feedforward control was implemented to mimic the open-loop control law, using a Causal Systems EZ-ANC II. The control filters were FIR with 150 taps (for more information on

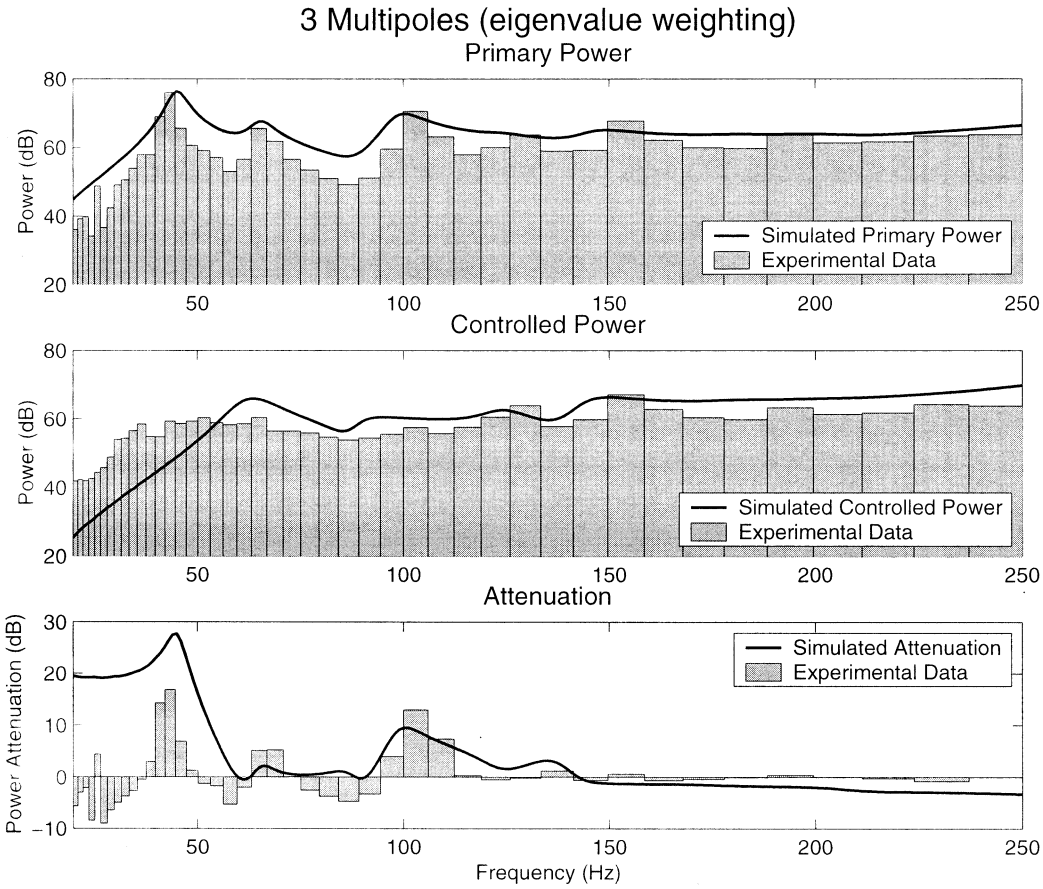

Fig. 10. Power attenuation achieved minimizing three multipoles.

adaptive feedforward control, see [33]). The inbuilt modal filtering capabilities of the EZ-ANC II enabled weighted combinations of the accelerometer signals to be used as error criteria. All of the input (accelerometer) signals were multiplied by a numerical weight and summed together to form an error criteria. The weights were calculated to incorporate the $\mathbf{H}$, $\mathbf{Q}$, and $\mathbf{\Lambda}$ terms from (25). Note that, as in the simulations, the weightings used were only correct at 100 Hz, but, by using these weights, no filtering was required to deal with the frequency dependence of the multipole combinations and their radiation efficiencies. Consequently, each error signal fed to the adaptive algorithm corresponded to a multipole combination. The number of multipoles to be minimized was chosen by selecting the active number of error signals being fed to the algorithm.

The sound power radiated by the panel was estimated by measuring the sound intensity on a 100 mm (x direction) by 100 mm (y direction) grid of points on a plane 200 mm above the surface of the panel. This resulted in the sound intensity being measured at 15 points in the x direction and nine points in the y direction and a 1.4 m $\times$ 0.8 m measurement plane (slightly larger than the panel). The sound intensity measurements were made in 12th octave bands and the measurement process was automated using a computer-controlled traverse integrated with a Bruel and Kjaer PULSE system. Note that this method only approximately measures the sound power radiated by the panel as some of the sound radiated by the panel would have not have been radiated perpendicular to the panel surface and so would have not been recorded on the measurement plane.

A photograph of the experimental panel is provided in Fig. 9. The panel is shown in its steel base with the eight accelerometers attached to it. The grid, drawn in black, on the panel surface represents the grid of points above the panel at which the intensity was measured.

With the primary force operating in isolation, the acoustic intensity was measured at all points above the panel. The intensity measurements were integrated to give the approximate radiated acoustic power from the panel. Control was then implemented and the intensity at all points above the panel were remeasured and the power radiated by the plate recalculated. The amount of attenuation achieved using a particular method of control was calculated by comparing the controlled power level to the primary power level.

B. Results

Fig. 10 shows the attenuation that was achieved when the amplitude of three multipole combinations were resolved by the modal filtering arrangement and attenuated by the controller. Shown in Fig. 11 is a similar result, where only one multipole combination is resolved. Simulated results are also shown for comparison.

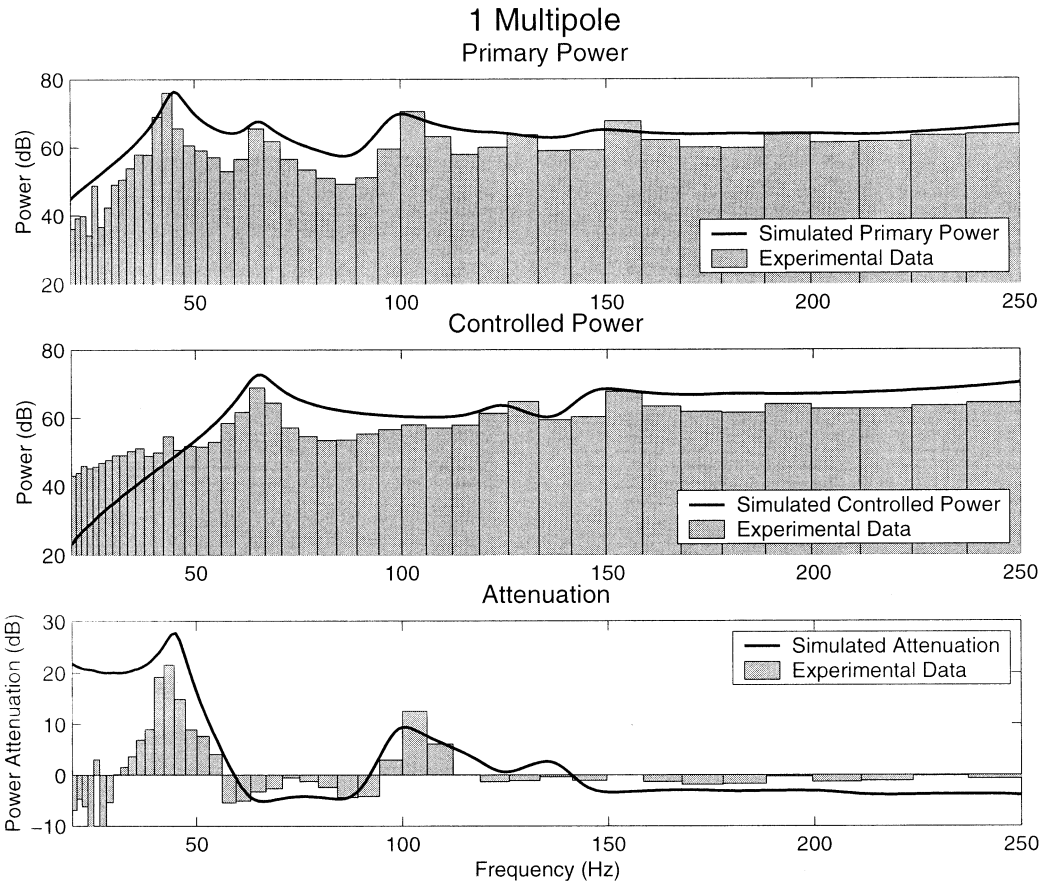

Fig. 11. Power attenuation achieved minimizing one multipole.

Observe that there was good correlation between the experimental results and those obtained from simulation. As would be expected when using a global error criterion, a large reduction in the power associated with the resonance peaks was obtained of approximately 20 dB for the first peak. When one multipole is minimized, the attenuation of the first peak in the power spectrum is greater than when three multipoles are minimized. This is because in the former case all of the control effort is focused on the first peak in the power spectrum (which corresponds to the first multipole), whereas in the latter case the control effort is distributed across the first three peaks (corresponding to the first three multipoles).At higher frequencies, the maximum possible attenuation using only one control shaker is very low (see Fig. 7), and this is evident in the experimental results.

It can be seen in Figs. 10 and 11 that the experimental attenuation at very low frequencies (i.e., less than approximately 30 Hz) was less than predicted in the simulation. The amount of attenuation at these frequencies was not expected to be very large for a number of practical reasons. First, the accuracy of the cancellation path transfer function estimate used in the adaptive algorithm [33] would be questionable at such frequencies. Second, with a sample rate of 5208 Hz, it would be expected that performance at frequencies below a few tens of Hertz would be poor [4]. Additionally, $1/f$ noise from the sensing system will impede the adaptive algorithm at very low frequencies. The general roll-off of results at low frequencies is not uncommon.

Shown in Fig. 12 are the results obtained when three multipoles were minimized, neglecting the eigenvalue weighting $\mathbf{\Lambda}$ of the groupings of multipoles. As can be seen, the results were not greatly affected in this instance. Modal filtering alone produces a satisfactory result.

Finally, it must be emphasized again that, when considering the results shown here, the objective was to develop a new sensing strategy and show that a good representation of acoustic power can be obtained with a very limited number of outputs from the sensing system. No effort was made to optimize the type of control law used, and in fact this sensing strategy could be adapted to be used with a range of control laws.

VI. Conclusion

A new sensing system design strategy has been presented that enables a modal filtering-type exercise to be performed on the acoustic field radiated by a structure, without knowledge of the structural mode shape functions. The radiation patterns produced by acoustic multipoles were used as a basis to describe the sound field, and a method was presented for calculating the appropriate weights to be applied to an array of structural sensor signals to resolve the multipole amplitudes.

To demonstrate the effectiveness of such a sensing system, simulated and experimental results were presented for sensing and then controlling (using adaptive feedforward control) the

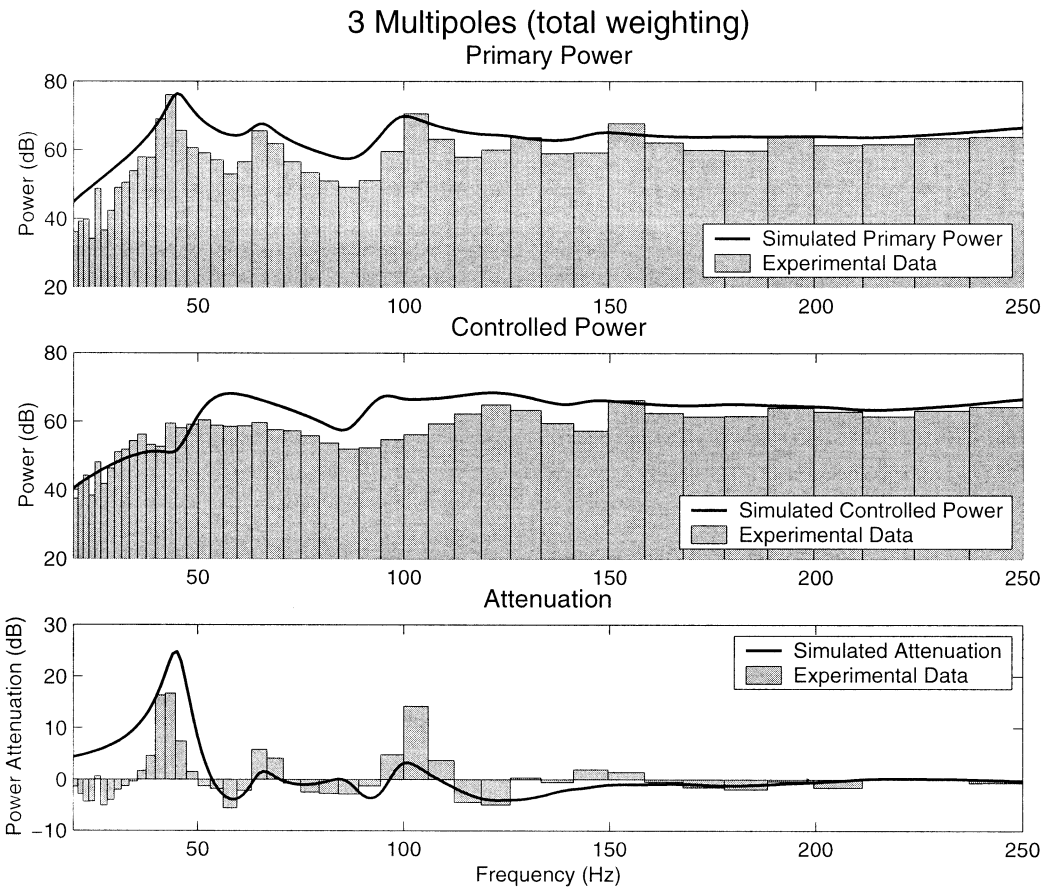

Fig. 12. Power attenuation achieved minimizing three multipoles, neglecting eigenvalue weighting.

sound power radiated by a rectangular panel. There was excellent correlation between the simulated and experimental results. The results indicate that the output from such a sensing system gives an accurate representation of a global error criterion and can be used by a control system to produce a global result with a minimum number of inputs to the control law and tuning algorithm.

REFERENCES

[1] W. B. Conover, "Fighting noise with noise," *Noise Control Eng. J.*, pp. 78–82, 1956.

[2] T. Berge, O. Kr. O. Pettersen, and S. Sorsdal, "Active noise cancellation of transformer noise," in *Proc. Inter Noise*, 1987, pp. 537–540.

[3] T. Berge, O. Kr. O. Pettersen, and S. Sorsdal, "Active cancellation of transformer noise: Field measurements," *Appl. Acoust.*, vol. 23, pp. 309–320, 1988.

[4] S. D. Snyder, "Active control—A bigger microprocessor is not always enough," *Noise Control Eng. J.*, vol. 49, pp. 21–29, 2001.

[5] L. Meirovitch and H. Baruh, "Control of self-adjoint distributed-parameter systems," *AIAA J.*, vol. 5, no. 1, pp. 60–66, 1982.

[6] ——, "The implementation of modal filters for control of structures," *AIAA J. Guid., Contr. Dynam.*, vol. 8, no. 6, pp. 707–719, 1985.

[7] D. R. Morgan, "An adaptive modal-based active control system," *J. Acoust. Soc. Amer.*, vol. 89, no. 1, pp. 248–256, 1991.

[8] C. K. Lee and F. C. Moon, "Modal sensors/actuators," *J. Appl. Mech.*, vol. 57, pp. 434–441, 1990.

[9] G. V. Borgiotti, "The power radiated by a vibrating body in an acoustic fluid and its determination from boundary measurements," *J. Acoust. Soc. Amer.*, vol. 88, no. 4, pp. 1884–1893, 1990.

[10] S. D. Snyder and N. Tanaka, "On feedforward active control of sound and vibration using vibration error signals," *J. Acoust. Soc. Amer.*, vol. 94, no. 4, pp. 2181–2193, 1993.

[11] S. J. Elliott and M. E. Johnson, "Radiation modes and the active control of sound power," *J. Acoust. Soc. Amer.*, vol. 94, no. 4, pp. 2194–2204, 1993.

[12] S. D. Snyder, N. Tanaka, and Y. Kikushima, "The use of optimally shaped piezo-electric film sensors in the active control of free field structural radiation, Part 1: Feedforward control," *ASME J. Vibr. Acoust.*, vol. 117, pp. 311–322, July 1995.

[13] ——, "The use of optimally shaped piezo-electric film sensors in the active control of free field structural radiation, Part 2: Feedback control," *ASME J. Vibr. Acoust.*, vol. 118, pp. 112–121, Jan. 1996.

[14] A. J. Kempton, "The ambiguity of acoustic sources—A possibility for active control?," *J. Sound Vibration*, vol. 48, no. 4, pp. 475–483, 1976.

[15] G. H. Koopmann, L. Song, and J. B. Fahnline, "A method for computing acoustic fields based on the principle of wave superposition," *J. Acoust. Soc. Amer.*, vol. 86, no. 6, pp. 2433–2438, 1989.

[16] J. S. Bolton and T. A. Beauvilain, "Multipoles sources for cancellation of radiated sound fields," *J. Acoust. Soc. Amer.*, vol. 91, p. 2349 (A), 1992.

[17] T. A. Beauvilain and T. S. Bolton, "Cancellation of radiated sound fields by the use of multipole secondary sources," in *Proc. 2nd Conf. Recent Advances in Active Control of Sound and Vibration*, Lancaster, PA, 1993, pp. 957–968.

[18] J. S. Bolton, B. K. Gardner, and T. A. Beauvilain, "Sound cancellation by the use of secondary multipoles," *J. Acoust. Soc. Amer.*, vol. 98, no. 4, pp. 2343–2362.

[19] T. A. Beavilain, "Multipole sources for the active control of radiated sound fields," Ph.D. dissertation, Sch. Mech. Eng., Purdue Univ., West Lafayette, IN, 1993.

[20] S. G. Hill, S. D. Snyder, and B. S. Cazzolato, "A generalized approach to modal filtering for active noise control: Acoustic sensing," *IEEE Sensors J.*, vol. 2, Dec., 2002.

[21] S. D. Snyder, N. C. Burgan, and N. Tanaka, "An acoustic-based modal filtering approach to sensing system design for active control of structural acoustic radiation: Theoretical development," *Mech. Syst. Signal Process.*, vol. 16, no. 1, pp. 123–139, Jan. 2002.

[22] E. F. Crawley and J. D. Luis, "Use of piezoelectric actuators as elements of intelligent structures," *AIAA J.*, vol. 25, no. 10, pp. 13373–11385, 1987.
[23] E. F. Crawley, "Intelligent structures for aerospace: A technological overview and assessment," *AIAA J.*, vol. 32, no. 8, pp. 1689–1699, 1994.
[24] R. L. Clark and C. R. Fuller, "Control of sound radiation with adaptive structures," *J. Intell. Mater. Syst. Struct.*, vol. 2, pp. 431–452, 1991.
[25] H. F. Harmuth, *Transmission of Information by Orthogonal Functions*, 2nd ed. Berlin, Germany: Springer Verlag, 1972.
[26] R. J. Pinnington and D. C. R. Pearce, "Multipole expansion of the vibration transmission between a source and a receiver," *J. Sound Vibr.*, vol. 142, no. 3, pp. 461–479, 1990.
[27] S. S. Agaian, *Hadamard Matrices and Their Applications*, ser. Lecture notes in mathematics; 1168. Berlin, Germany: Springer-Verlag, 1985.
[28] S. D. Snyder and N. Tanaka, "Calculating total acoustic power output using modal radiation efficiencies," *J. Acoust. Soc. Amer.*, vol. 97, no. 3, pp. 1702–1709, 1995.
[29] B. D. O. Anderson and J. B. Moore, *Optimal Control, Linear Quadratic Methods Methods*. Englewood Cliffs, NJ: Prentice-Hall, 1990.
[30] W. Baumann, F.-S. Ho, and H. H. Robertshaw, "Active structural acoustic control of broadband disturbances," *J. Acoust. Soc. Amer.*, vol. 92, pp. 1998–2005, 1992.
[31] N. K. Gupta, "Frequency-shaped loop functionals: Extensions of linear quadratic Gaussian design methods," *J. Guid. Contr.*, vol. 3, pp. 529–535, 1980.
[32] J. C. Nash, "Compact numerical methods for computers: Linear algebra and function minimization," in *Real Symmetric Matrices*. Bristol, U.K.: Adam Hilger, 1979, ch. 10.
[33] C. H. Hansen and S. D. Snyder, *Active Control of Noise and Vibration*. London, U.K.: E&FN Spon, 1997.
[34] J. Pan, S. D. Snyder, C. H. Hansen, and C. R. Fuller, "Active control of far-field sound radiated by a rectangular panel—A general analysis," *J. Acoust. Soc. Amer.*, pt. 1, vol. 91, no. 4, pp. 2056–2067, Apr. 1991.
[35] S. D. Snyder, N. Tanaka, K. Burgemeister, and C. H. Hansen, "Direct-sensing of global error criteria for active noise control," in *Proc. Active 95*, 1995, pp. 849–860.
[36] S. D. Snyder, "Microprocessors for active control: Bigger is not always enough," in *Plenary Address Proc. Active 99*, 1999, pp. 45–62.

Nicholas C. Burgan received the B.E. degree (hons.) in mechanical engineering from the University of Adelaide, Adelaide, Australia, in 1999. He is currently working toward the Ph.D. degree in engineering at the same university.

He is working on active noise, vibration, and active structural acoustic control as a member of the Active Noise and Vibration Control Group at the Department of Mechanical Engineering, University of Adelaide.

Scott D. Snyder received the Ph.D. degree in mechanical engineering from the University of Adelaide, Adelaide, Australia, in 1991.

During 1992 he worked at the Mechanical Engineering Laboratory, Tsukuba Science City, Japan. From 1993 to 2000, he worked in the Department of Mechanical Engineering, University of Adelaide, first as a research officer, then as an academic. In 2000, he moved to the position of General Manager, Information Technology Services. His research interests include active noise and vibration control, control systems, and signal processing. He is the author or coauthor of two books and 40 journal papers in this area.

Nobuo Tanaka received the M.S. and Ph.D. degrees in mechanical engineering from Tokyo Metropolitan University, Tokyo, Japan, in 1973 and 1977, respectively.

From 1975 to 1976, he was on study leave at the University of California at Berkeley. From 1976 to 1998, he worked as a Research Scientist at the Mechanical Engineering Laboratory in Japan. During 1994, he was a visiting academic at the University of Adelaide, Adelaide, Australia. Since 1998, he has been a Professor in the Mechanical Engineering Department, Tokyo Metropolitan Institute of Technology. His research interests include theory and implementation of active noise and vibration systems.

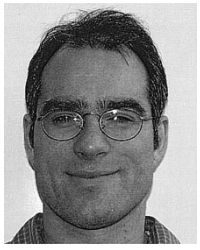

Anthony C. Zander received the B.E. degree (hons.) and the Ph.D. degree from the University of Adelaide, Adelaide, Australia, in 1989 and 1994, respectively.

From 1994 to 1998, he worked as a Research Engineer in the Noise and Flow Control Group of United Technologies Research Center (UTRC), East Hartford, CT, where he developed analytical models and conducted experimental investigations on active and passive noise and vibration control applied to a variety of products. From 1998 to 1999, he worked as a Senior Engineer with Vipac Engineers and Scientists. He is currently a Senior Lecturer in the School of Mechanical Engineering, University of Adelaide, and his research interests include modeling and experimental analysis of active and passive control of noise and vibration.